

---

## **A New Gas-Phase Analytical Tool**

---

**Sieghard Albert, Douglas T. Petkie, Ryan P. A. Bettens,  
Sergei P. Belov and Frank C. De Lucia**

Ohio State University

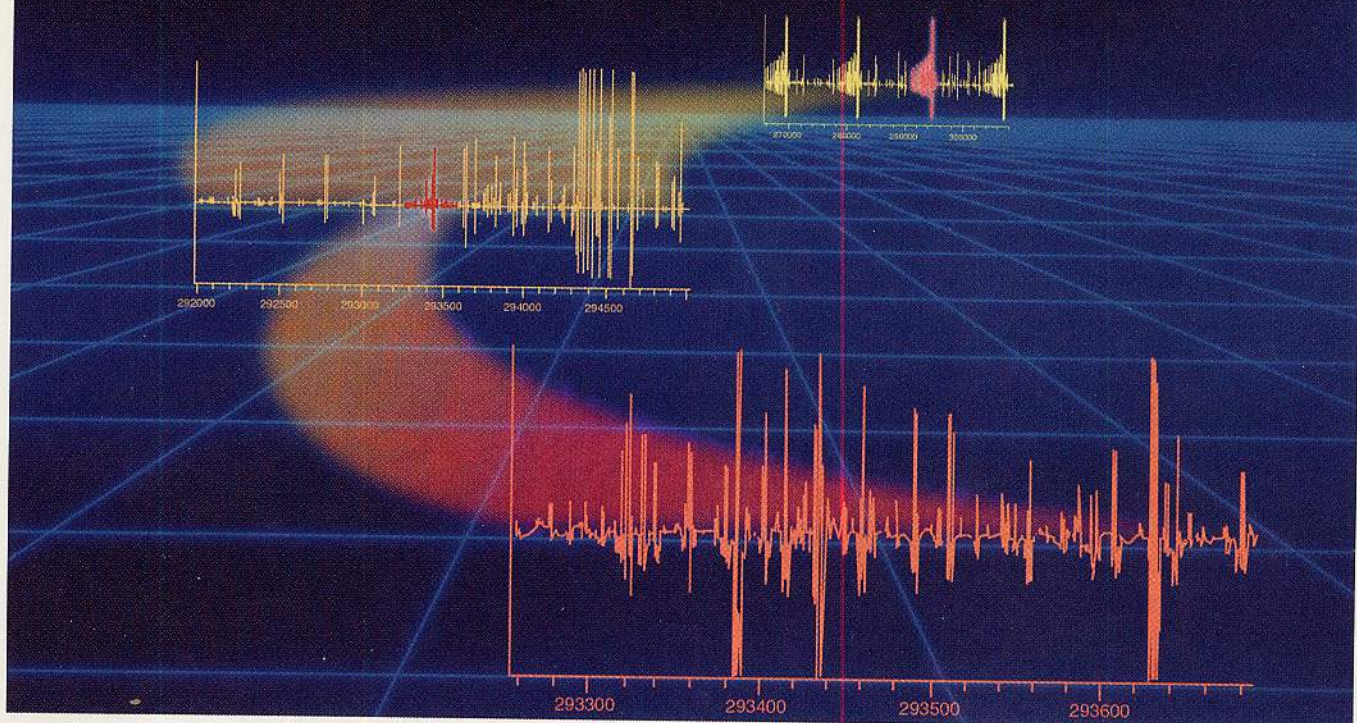
# **ANALYTICAL CHEMISTRY NEWS & FEATURES**

Reprinted from  
Volume 70, Number 21, Pages 719A-727A

Sieghard Albert  
Douglas T. Petkie  
Ryan P. A. Bettens  
Sergei P. Belov  
Frank C. De Lucia  
Ohio State University



## FASSST: A New Gas-Phase Analytical Tool



GH MULTIMEDIA

*Fast-scan submillimeter spectroscopy technique offers general analytical utility, speed, and detection capability.*

Almost from the beginning, microwave spectroscopy's potential for the chemical analysis of gases that can be collected in a low-pressure cell has been recognized (1). Although techniques based on the UV, optical, and IR regions of the electromagnetic spectrum have become standard analytical tools (2, 3), this early promise has not been realized at longer wavelengths. In the late 1950s and early 1960s, a commercial instrument, operating in the frequency region of 10–40 GHz was developed and marketed by Hewlett-Packard. This instrument, sold primarily to spectroscopists with interests in molecular structure, experienced only modest commercial success within the analytical community because of its large size, high cost, and complexity.

The fast-scan submillimeter spectroscopy technique (FASSST) described in this Instrumentation overcomes these limitations and also offers significantly greater general analytical utility, speed, and detection capability. FASSST is based on the last part of the electromagnetic spectrum, the submillimeter (100–1000 GHz,  $3.3\text{--}33\text{ cm}^{-1}$ ,  $3.0\text{--}0.3\text{ mm}$ ), which has not been used widely for analytical purposes. In this spectral region, fingerprints arise from the rotational energy levels of molecules. These

**Sieghard Albert**  
**Douglas T. Petkie**  
**Ryan P. A. Bettens**  
**Sergei P. Belov**  
**Frank C. De Lucia**  
 Ohio State University



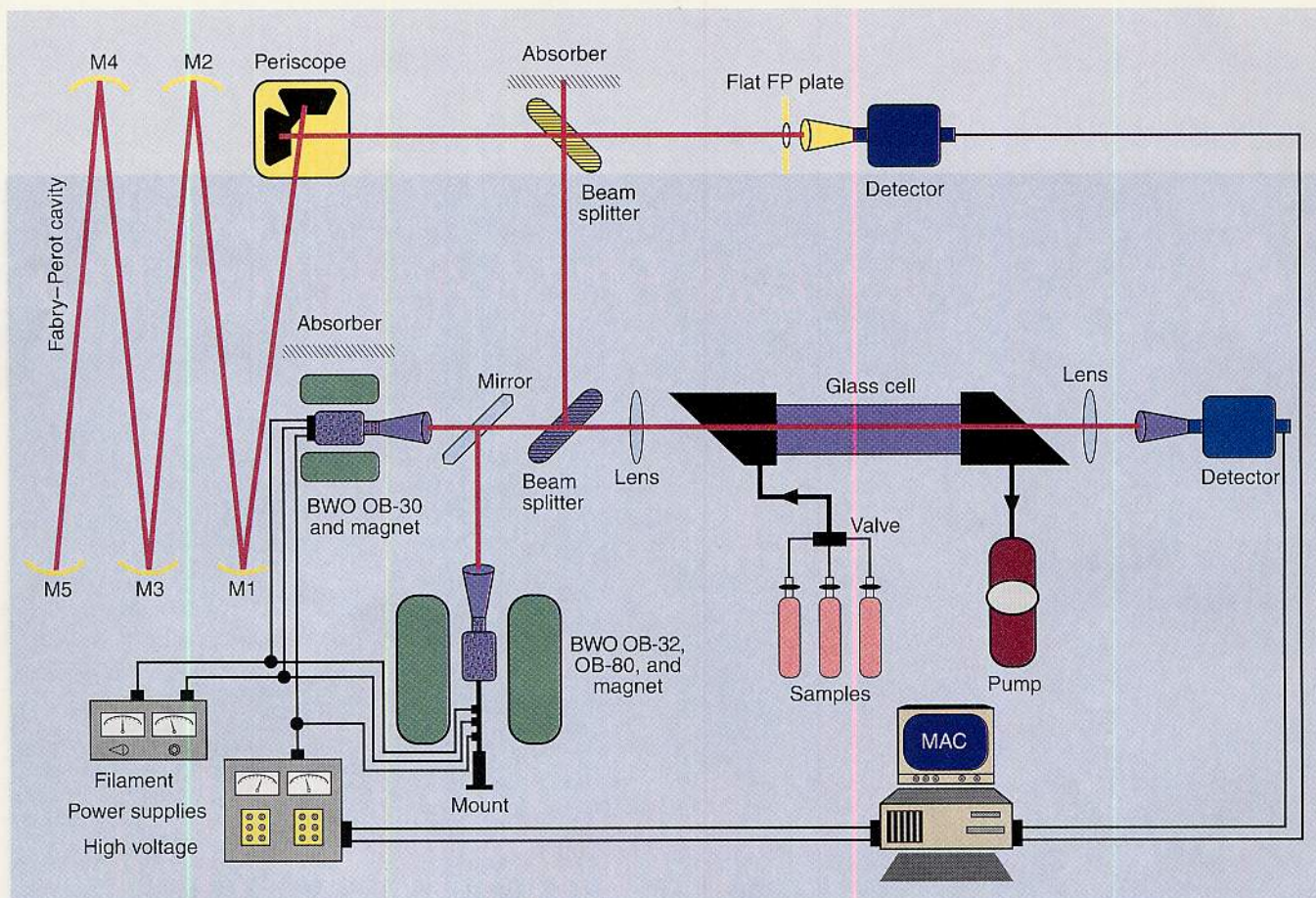


**Figure 1. Layout of the FASSST system.**

M1–5 are mirrors. OB-30, 32, and 80 are types of BWOs.

fingerprints are ordinarily complex and unique because many rotational levels are thermally populated. Additionally, the underlying physical interactions between radiation and matter are strong, and, at low pressure, the Doppler broadening is small, which allows high resolution.

The FASSST methodology is fundamentally simple and powerful. It is based on electronically tunable sources of high spectral brightness and spectral purity. Fast scanning, "optical" calibration, and modern data-acquisition and computational techniques replace the more complex phase-lock techniques ordinarily used. We will show how these advances make it possible for FASSST to take its place alongside analytical techniques that have been developed at shorter wavelengths.

Although the difficulties of developing appropriate technology in the submillimeter spectral region have, until now, pre-

cluded its development for general analytical purposes, the underlying physics is very favorable. Briefly stated, the FASSST system is orders-of-magnitude more sensitive than systems operating in the adjacent microwave region. It is significantly faster and less complex than other submillimeter systems and provides absolute quantitative analysis traceable to fundamental theory and/or straightforward calibration. FASSST provides orders-of-magnitude greater resolution and requires smaller samples than IR systems, especially those of comparable size and complexity. The greater resolution and smaller sample results from the much smaller Doppler width in the submillimeter, which makes the optimum sample pressure for sensitivity and resolution 10–100 mTorr.

The opening act is a spectrum of nitric acid, a molecule of moderate size and

spectral complexity, which can be used to illustrate the nature of FASSST's submillimeter rotational spectra. Because a single FASSST scan contains  $\sim 10^6$  frequency-resolution elements, it is not possible to graphically display a complete, full-band spectrum. Consequently, the spectrum shows a series of enlargements in frequency and sensitivity, which provides a good perspective. The 45-GHz scan shown at the top was recorded in a single 1-s scan, and the 300-MHz scan at the bottom was recorded in 0.01 s.

### The system

The FASSST system, shown in Figure 1, is simple in concept and straightforward in execution. Its power is derived from the physics that govern molecular interactions in the submillimeter range (Box on p. 724 A) and from modern computational techniques that coordinate and exploit the



system's capabilities. In this example, a backward wave oscillator (BWO) tube (ISTOK OB-30) is used to cover the 240–375 GHz region (www.ISTOK.com). Similar tubes are available for the 100–1000 GHz region. The beam splitter splits the output power of the BWO, with 90% directed quasi-optically through the molecular absorption cell of 1–10 m length and detected by a 4K InSb hot-electron bolometer (4). In this configuration, a 10-cm diameter glass cell (common drain line) with polyethylene windows was used. Metal tubing of 1–2 cm diameter is also commonly used. The remaining 10% of the power is coupled into a Fabry–Perot (FP) cavity via a second beam splitter, which provides fringes for frequency interpolation between reference spectral lines of known frequency.

To maximize the dynamic range of the spectrum, the low-frequency response of the analog amplifiers between the detector and the A/D input to the computer is adjusted to provide an approximately first derivative lineshape and to generally suppress the recording of the power variations of the BWO and multipath interference effects. The convolution of the recorded first derivative lineshape with a reference first derivative lineshape in the signal-processing software results in the approximately second derivative lineshape shown in the opening art on p. 719 A, a FASSST spectrum of nitric acid. For the study of weaker lines, additional analog gain is used at the expense of the measurement of the amplitude of the stronger lines. In the current system (which is not optimized for sensitivity), strongly absorbing lines have a S/N of  $10^4$  in 1 MHz of bandwidth (1  $\mu$ s of integration time). Comparisons of spectra obtained on phase-locked systems with FASSST spectra show that they too are Doppler-limited.

In this Instrumentation, we will provide an overview of those aspects most important for analytical systems, namely the characteristics of the BWO submillimeter source and the optical frequency calibration scheme. Additional details are provided elsewhere (5).

Two requirements are necessary for the BWO sources for a FASSST system. The first and most important requirement is that the spectral width of the source, aver-

aged over the time required to sweep through the line (typically  $10^{-5}$  s) be much less than the sample's spectral linewidths. Studies done over many years have shown that the short-term width of free-running BWOs is <20 kHz (6) and Doppler widths near 300 GHz are  $\sim 1$  MHz, easily meeting this requirement. The second requirement is that the sources be voltage-tunable over a 50% frequency range. This tunability is necessary for the desired spectral coverage and for the optical calibration scheme used. This range contains  $\sim 10^5$  spectral-resolution elements (Doppler-limited) and  $\sim 10^6$  distinct measurable line frequencies. For most molecules of analytical interest, 100–10,000 of the resolution elements will be filled with strong, fully resolved "fingerprint" lines.

The BWO is a classical device in which a beam of electrons interacts with a periodic slow-wave structure, which supports the propagation of an electromagnetic wave in the opposite direction (7–9). To accomplish a net transfer of energy from the electrons to the electromagnetic wave and support oscillation, the electrons must be bunched and the interaction between the bunches and the wave organized so that the bunches always interact with a phase of the wave that produces deceleration. Because the electron velocity has a first-order effect in this phase relationship, the frequency of oscillation is strongly dependent on the electric potential between the cathode and slow-wave structure, thus providing broad electrical tunability.

To maintain the required phasing, the spatial periodicity of the slow-wave structure must be on the scale of the distance

traveled by the electron bunch in one oscillation of the electromagnetic wave. For an accelerating voltage of a few thousand volts and  $\lambda = 1$  mm, this distance is  $\sim 100 \mu$ m. Although this is large by modern microfabrication standards, energy-handling capabilities decrease and circuit losses increase rapidly with decreasing wavelength and circuit size. As a result, the manufacture of BWOs and other electron beam tubes for  $\lambda < 1$  mm has been a challenge. Nevertheless, in spite of these small dimensions and highly energetic electron beams, years of development work on these sources have resulted in a high level of reliability for the BWOs used in this work. In three years of operation ( $\sim 1000$  hours), we have not had a BWO burn out or experienced any noticeable deterioration in performance. This result is consistent with the experience of others.

The high spectral purity and frequency tunability of BWOs can be exploited only in the context of a power supply and calibration scheme with complementary properties. Typically, a BWO tunes over a range of 100 GHz with a voltage variation of  $\sim 2000$  V, a tuning rate of 50 MHz/volt. If it is desired that the voltage fluctuations of the power supply result in a frequency variation which is no more than 10% of a linewidth, then the fluctuations must be less than 2 mV in the context of a power supply capable of sweeping several thousand volts. We have developed such a power supply (5). Alternatively, for the somewhat relaxed frequency calibration requirements of many analytical applications and/or for very fast scans, numerous simple commercial power supplies are satisfactory. Specifically, in a typical FASSST scan  $\sim 10^4$  Fabry–

**Table I. Detection limits for 1-s integration time.**

| Molecule                        | Absorption coefficient (cm <sup>-1</sup> ) | Detectable sample (moles) | EPL = 1 m               |                | EPL = 100 m             |                |
|---------------------------------|--|---------------------------|-------------------------|----------------|-------------------------|----------------|
|                                 |  |                           | Partial pressure (Torr) | Dilution (ppm) | Partial pressure (Torr) | Dilution (ppm) |
| HCN                             | 1  | $10^{-18}$                | $10^{-11}$              | 0.001          | $10^{-13}$              | 0.00001        |
| OCS                             | $10^{-1}$                                  | $10^{-17}$                | $10^{-10}$              | 0.01           | $10^{-12}$              | 0.0001         |
| SO <sub>2</sub>                 | $10^{-2}$                                  | $10^{-16}$                | $10^{-9}$               | 0.1            | $10^{-11}$              | 0.001          |
| CH <sub>3</sub> Cl              | $10^{-2}$                                  | $10^{-16}$                | $10^{-9}$               | 0.1            | $10^{-11}$              | 0.001          |
| HNO <sub>3</sub>                | $10^{-3}$                                  | $10^{-15}$                | $10^{-8}$               | 1.0            | $10^{-10}$              | 0.01           |
| CO                              | $10^{-3}$                                  | $10^{-15}$                | $10^{-8}$               | 1.0            | $10^{-10}$              | 0.01           |
| C <sub>4</sub> H <sub>5</sub> N | $10^{-3}$                                  | $10^{-15}$                | $10^{-8}$               | 1.0            | $10^{-10}$              | 0.01           |
| C <sub>5</sub> H <sub>5</sub> N | $10^{-3}$                                  | $10^{-15}$                | $10^{-8}$               | 1.0            | $10^{-10}$              | 0.01           |



Perot fringes/s are recorded. Because the resulting 100  $\mu$ s between calibration points is much less than the period of power supply ripple, thermal drift, and typical pick-up, these instabilities are "frozen" and compensated for in the calibration software (discussed later). For example, the spectrum in the opening art was obtained with a simple Bertan 210-05R switching power supply.

In a FASSST system, the synthesized frequency reference and phase lock typical of high-resolution submillimeter spectrometers is replaced by a system more typical of optical spectrometers. If the frequency of a BWO as a function of voltage were linear, the frequency calibration scheme could be as simple as having two spectral lines of known frequency somewhere near the opposite ends of the frequency sweep range and using linear interpolation. However, the small-scale structure is much more complex, and if the effects of this small-scale structure are not properly treated, the frequency accuracy of the FASSST system will be  $\sim 100$  MHz, approximately 1000 times worse than that required for high-resolution spectroscopy and 100 times worse than is desirable for analytical applications. However, with a small FP mode spacing ( $\sim 5$  MHz) it is possible to use simple linear interpolation methods to measure line frequencies to 10% of the Doppler limited linewidth (5).

Based on these considerations, the basic FASSST calibration scheme is designed to take a fast ( $10^4$ – $10^5$  MHz/s) scan over the spectral region of interest; include two or more (typically 50+ are available) reference lines; use the known frequencies of the reference lines to determine the FP cavity mode spacing and absolute frequency; count FP modes to establish the frequency of each fringe; and use linear interpolation between the two nearest FP modes to calculate molecular absorption frequencies.

Although the accounting of costs associated with technological development can vary widely, it is useful to discuss the cost of the system described above and the cost of related, more specialized analytical systems that might be built. The cost of BWOs varies with frequency band but is on the order of \$10,000. The Bertan power supply used to produce the spectrum in the open-

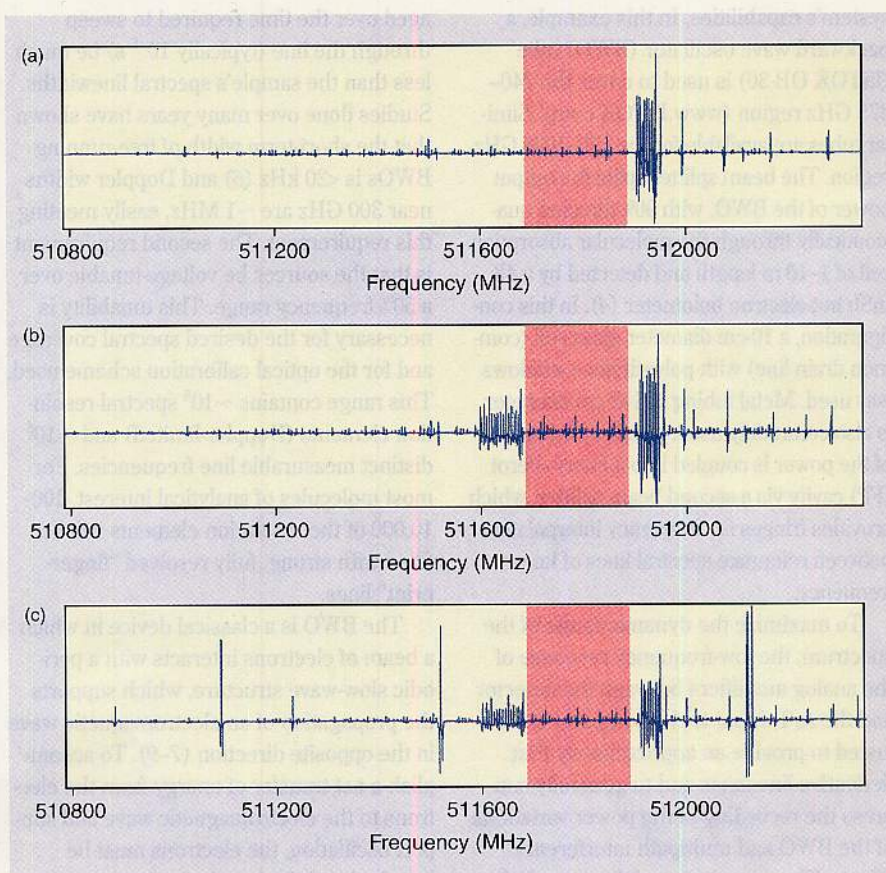


**Figure 2. Spectrum of 1 GHz around 512 GHz which results from the successive addition of (a) 10 mTorr of pyrrole, (b) 20 mTorr of pyridine, and (c) 20 mTorr of sulfur dioxide.**

ing art cost \$2500, as did the components of the more elaborate sweeping power supply described earlier. The helium-based detectors cost \$10,000 each. The remaining optics, spectroscopic cell, and so on, cost \$2000. The costs of a data-acquisition system, vacuum pumps, and so on, are not included here because they vary widely and are largely dependent on local preferences.

It is important that other more specialized versions of FASSST could be very inexpensive, especially in quantity. This factor is especially true for versions that take advantage of solid-state microwave components, which are a product of the rapid expansion of wireless communication into the millimeter spectral region. At present, these systems would be less capable than the system described above, but they can satisfy the requirements of many analytical applications and are perhaps already an order-of-magnitude less costly.

### Spectroscopy in the submillimeter

Figure 2 shows the FASSST spectra obtained with an OB-80 BWO in the 1 GHz region near 512 GHz, which results from first adding 10 mTorr of pyrrole to the sample cell (upper trace), then 20 mTorr of pyridine (middle trace), and finally 20 mTorr of  $\text{SO}_2$  (lower trace). Figure 3 shows an expansion of the 0.2 GHz shaded region near 511.8 GHz. The spectrum in Figure 3 is 0.1% of the BWO bandwidth and represents 0.01 s of data acquisition. In each figure, the sensitivity is such that no noise can be displayed on the graph. The lines in the top trace of each figure are Doppler limited, whereas those in the middle and lower trace show modest pressure broadening.

Pyrrole and pyridine are molecules of intermediate size and weight and show both regions of widely spaced lines as well as more compact features. It is clear even in the small expanded spectral interval dis-



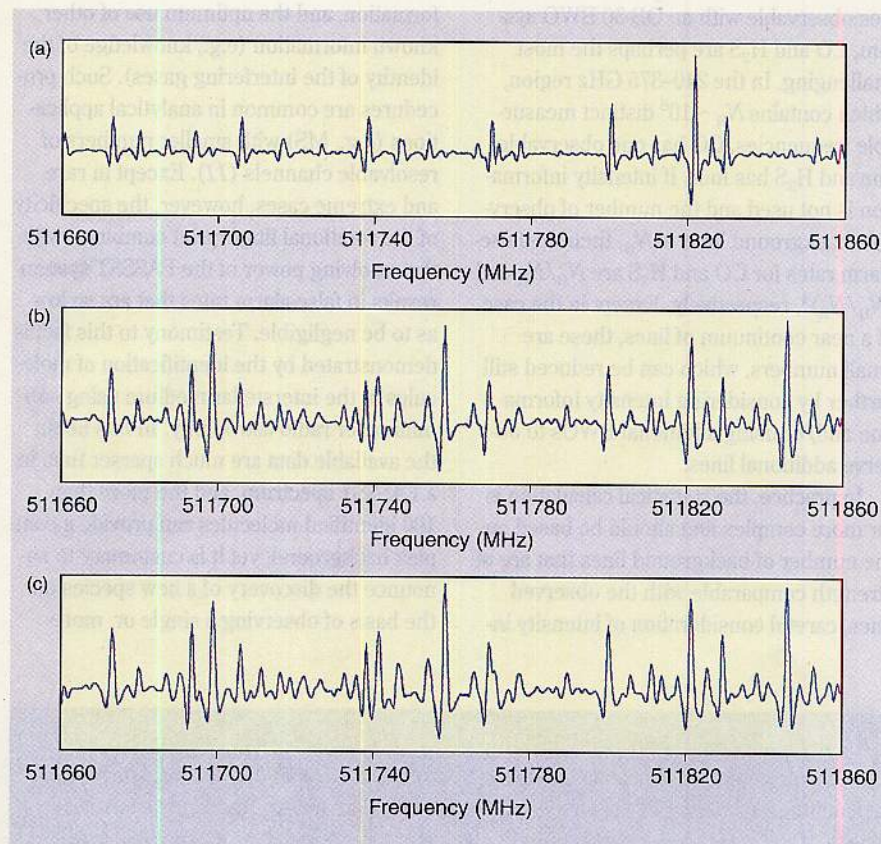


**Figure 3. Expansions of the 0.2 GHz shaded regions near 511.8 GHz shown in Figure 2. Each scan required about 0.01 s of data acquisition and represents about 0.1% of the full range of a BWO.**

played in the figure that each has a unique signature, as they would in almost any other randomly chosen small interval throughout the submillimeter. On the other hand,  $\text{SO}_2$  has only about six strong lines in the 1-GHz region near 512 GHz and none in the smaller 0.2-GHz expanded region. A region that contains a few of  $\text{SO}_2$ 's several hundred strong submillimeter lines must be selected for its identification and quantitative measurement.

**Sensitivity.** The FASSST system described here operates at frequencies that are 10–100 times higher than the region historically referred to as the microwave. The distinction between systems operating in the microwave and the submillimeter regions is very important. As discussed in the box on p. 724 A, molecular absorption strengths increase with frequency with a functional dependence of  $\nu^2$ – $\nu^3$ , peaking somewhere in the submillimeter region. As a result, spectroscopic systems in this region are  $10^2$ – $10^6$

more sensitive than the much more common microwave systems. Additionally, the larger bandwidth of the submillimeter in comparison to the microwave results in virtually universal coverage of molecular species, subject only to the requirement that the species have a dipole moment or a large amplitude vibration in the submillimeter. The only chemically stable species that is an exception is HF (1200 GHz). HCl (600 GHz), HBr (500 GHz), and  $\text{NH}_3$  (600 GHz) are not observable using an OB-30 BWO but can be measured with other BWOs (OB-32 at 370–535 GHz and OB-80 at 526–714 GHz).

Sensitivity comparisons with IR systems are more complex because of the diversity of IR technologies used for analytical purposes, as well as the variety of applications. The FASSST system is inherently very sensitive, however. It is based on the principle that powerful electronic oscillators are fundamentally very bright and very quiet, and that the rotational transition moments of

the submillimeter are related to the total electric dipole moment. In addition, at long wavelengths, it is possible to build very quiet detectors, and the noise caused by microphonics and such is much reduced.

Table 1 lists absorption coefficients typical for the stronger lines of several molecules of interest. In the current FASSST system, which uses 1  $\mu\text{s}$  of integration time, the S/N is  $10^4$ . Extensive experience with submillimeter spectrometers has shown that the full statistical gain associated with smaller bandwidths can be obtained to at least 1 s of integrating time, with longer integrating times often used. Table 1 also lists detection limits for a 1-s integration period, a fairly short period for most analytical applications. The S/N for an optically thin absorption line becomes the product of the 1-s integration time S/N ( $10^7$ ) times the absorption coefficient times the cell length. The minimum detectable partial pressure is then the optimum pressure (0.01 Torr) divided by the absorption S/N at optimum pressure. An absorption cell length of 1 m length is typical for submillimeter spectroscopy. For weak absorptions, long-path techniques can be used. Effective path lengths (EPLs) of 100 m can be achieved using Fabry Perot cavities or White-cell configurations. Dilution ratios are calculated relative to a nominal total pressure of 10 mTorr. In the Doppler limit, the minimum detectable sample depends upon the cell cross section, but not its length. In Table 1, the minimum detectable sample is calculated for a cell cross section of  $10^{-2} \text{ cm}^2$ , somewhat larger than fundamental waveguide  $\lambda$  at = 1 mm (300 GHz).

**Specificity and rotational spectroscopy.** The large number of resolvable channels in the submillimeter, the large number of thermally excited rotational lines that populate these resolvable channels, the high S/N attainable (even with very short integrating times), and the absolute measurement of absorption coefficients available in the submillimeter make it possible in virtually all scenarios to set false alarm rates that are so low as to be considered absolutely specific.

Because Doppler-limited lines for molecules with masses of 100 amu have line Q values of  $\sim 3 \times 10^5$  independent of spectral region, any Doppler-limited spectroscopic



instrument has  $10^5$  resolution elements in a 30% bandwidth ( $Q = \Delta \nu / \nu$ ). If the rotational line density is comparable with or greater than the Doppler width so that adjacent lines overlap, however, the spectral resolution that can be used for analytical purposes is reduced to that of the width of the unresolved rotational bands or their "features", rather than that of the Doppler width of the instrument itself. Even in Doppler-limited IR systems, this important transition occurs for molecules whose size and mass are greater than about that of  $\text{ClONO}_2$  (10).

From a specificity point of view, the most difficult species are those that have only a few rotational lines within the spectral coverage of the FASSST system or are embedded in a dense background of spectral lines of unknown origin. Of stable spe-

cies observable with an OB-30 BWO system, CO and  $\text{H}_2\text{S}$  are perhaps the most challenging. In the 240–375 GHz region, which contains  $N_R \sim 10^6$  distinct measurable frequencies, CO has one observable line and  $\text{H}_2\text{S}$  has four. If intensity information is not used and the number of observable background lines is  $N_B$ , then the false-alarm rates for CO and  $\text{H}_2\text{S}$  are  $N_B/N_R$  and  $(N_B/N_R)^4$ , respectively. Except in the case of a near continuum of lines, these are small numbers, which can be reduced still further by considering intensity information and/or using additional BWOs to observe additional lines.

In practice, the statistical calculation is far more complex and should be based on the number of background lines that are of strength comparable with the observed lines, careful consideration of intensity in-

formation, and the optimum use of other known information (e.g., knowledge of the identity of the interfering gases). Such procedures are common in analytical applications (e.g., MS) with smaller numbers of resolvable channels (11). Except in rare and extreme cases, however, the specificity of the rotational fingerprint combined with the resolving power of the FASSST system results in false-alarm rates that are so low as to be negligible. Testimony to this fact is demonstrated by the identification of molecules in the interstellar medium using submillimeter radio astronomy. In this field, the available data are much sparser than in a FASSST spectrum, and the more than 100 identified molecules can provide a complex background, yet it is customary to announce the discovery of a new species on the basis of observing a single or, more

## Rotational spectroscopy

### Absorption strengths

If the absorption coefficient of the submillimeter power  $P$  absorbed by the molecules in the cell is defined by

$$\alpha = -(1/P) (\Delta P / \Delta x) \quad (1)$$

(in which  $x$  is the position in the cell), in the microwave limit (in which  $h\nu \ll kT$ ), the peak absorption coefficient between two rotational levels  $m$  and  $n$  is

$$\alpha = 8\pi^2 N F_m v^2 \mu_{mn}^2 / 3ckT\Delta\nu \quad (2)$$

in which  $N$  is the number of molecules per unit volume  $F_m$  is the fraction in state  $m$ ,  $v$  is the rotational transition frequency,  $\Delta\nu$  is the line width, and  $\mu_{mn}$  is the dipole matrix element in units of charge times length, and  $c$  is the speed of light (14). The transition moment  $\mu_{mn}$  contains contributions from the components of the permanent dipole moment along each of the principal axes of the moment of inertia tensor, which determines the rotational selection rules.

For optimum sensitivity, the gas pressure is adjusted in proportion to frequency so that the Doppler and pres-

sure broadening contributions to the linewidth are equal and  $N/\Delta\nu$  is independent of frequency. Because of degeneracy and rotational partition function effects,  $F_m$  is often proportional to  $v$  until the declining Boltzmann population causes it to fall exponentially. These factors typically yield absorption coefficients which rise as the cube of the frequency to reach a maximum at some optimum frequency in the submillimeter before declining exponentially.

### Energy levels and transition frequencies

The rotational energy levels of a molecule result from the quantization of its rotational kinetic energy according to

$$E_r = (1/2) [(P_x^2/I_x) + (P_y^2/I_y) + (P_z^2/I_z)] \quad (3)$$

in which  $P_x$ ,  $P_y$ , and  $P_z$  are the components of molecular angular momentum and  $I_x$ ,  $I_y$ , and  $I_z$  are the components of the principal moments of inertia. Molecules have additional effects (e.g., centrifugal distortion, perturbations, and internal rotations) that significantly complicate the spectroscopy (14) but minimally affect analytical applications and will not be considered further.

The high specificity of FASSST arises from the fact that the rotational degrees of freedom are unique: Many levels are thermally populated, and the strong fundamental rotational transitions that arise from these levels are not associated with functional groups, which may be constituents of many similar molecules. Rather, the transitions depend on the global moment of inertia tensor  $\mathbf{I}$  of the molecule. Because submillimeter spectroscopy is sensitive to changes in each of the components  $I_x$ ,  $I_y$ , or  $I_z$  of  $<10^{-7}$ , each molecule has a unique signature if only a few lines of its rotational structure can be detected and measured.

### Rotational spectra

For the most general case of an asymmetric rotor, none of the components of inertia are equal, and the quantized rotational energy levels become

$$E = 1/2(B + C)J(J + 1) + [A - 1/2(B + C)]W_{Jr}(b_p) \quad (4)$$

in which  $A$ ,  $B$ , and  $C$  are constants inversely proportional to the components of the moment of inertia,  $J$  is the rotational quantum number, and  $W_{Jr}(b_p)$  is a complicated function related to the de-



typically, a few spectral lines (12, 13).

**Quantitative analysis.** Because the strengths of the molecular rotational transitions depend upon the permanent molecular dipole moment and angular momentum quantum mechanics, measured fractional absorption can be translated into absolute concentration by Equation 2 in the Box on the previous page and calculation of the partition function. Whereas rotational partition functions are straightforward to calculate, large molecules can have significant vibrational partition functions with significant contributions from largely unknown, low-lying vibrational modes. In these cases the calculations should be verified experimentally with known samples.

Most important, because of the high resolution of FASSST spectra, any of many isolated rotational lines ordinarily can be

used for quantitative purposes, thus providing massive redundancy and eliminating the possibilities of contributions from interfering and overlapping lines. For example, in the opening art, any of more than 100 lines could be used to determine the concentration. In real systems, moderate efforts at establishing the partition functions and fractional absorption of the submillimeter power should result in a quantitative uncertainty of ~10%, whereas 1% should be achievable for most species with modest effort.

### Possibilities

The system described above has been configured as a general-purpose laboratory instrument, with high-resolution spectroscopic capabilities. For many applications, modifications are appropriate.

For analytical purposes that require identification rather than state-of-the-art spectroscopic measurement, the frequency calibration requirements can be relaxed significantly, resulting in a smaller and more compact system. For example, frequency measurement accurate to a Doppler broadened linewidth would still leave  $10^5$  distinct channels for identification rather than the  $10^6$  channels of the system shown in Figure 1. This significantly reduces the power supply stability and FP size requirements. Additionally, for applications that do not require maximum sensitivity and spectral coverage, the system has an all solid-state analogue (FASSST-SS) based on chirped GUNN oscillators and Schottky diode detectors.

The sensitivity and selectivity of a FASSST system is optimal when the sam-

ple of asymmetry of the molecule and angular momentum projection quantum numbers (14). However, in the symmetric top limit (in which two of the rotational constants are equal),  $W_{J,K}(b_p) = K^2$  (in which  $K$  is the projection of  $J$  onto the molecular symmetry axis), and it is possible to use this relation along with the dipole selection rule  $J \rightarrow J+1$  to illustrate the general character of rotational spectra. In this symmetric top limit, it is straightforward to show that the values of  $J$  and  $v$  for which rotational lines are strongest are given by

$$J_{\text{opt}} \sim 5(T/B)^{1/2} \quad (5)$$

and

$$v_{\text{opt}} \sim 2B + 11(BT)^{1/2} \quad (6)$$

in which  $B$  is a rotational constant in gigahertz (14).

Figure 4 plots the absorption coefficients at 300 K for the  $K=0$  component of each  $J \rightarrow J+1$  transition for symmetric tops of various  $B$  values. For rigid symmetric tops, the  $K \neq 0$  components are degenerate with the  $K=0$  transitions, but for real molecules, the components are slightly (a few megahertz) displaced due to centrifugal distortion effects. For asymmetric tops, the  $K \neq 0$  components

are more widely spread according to their asymmetry and Equation 4, but, on average, they have similar transition strengths. Additionally, because of the lower symmetry of asymmetric rotors, components of the dipole moment can exist along each axis, and a new set of selection rules and spectra will appear for each. Although this can lead to a spectrum of great complexity, the character of the symmetric tops is representative of the average spectral density, distribution in frequency, and strength of lines. The complete spectral assignment of asymmetric rotors can be a complex task, but from an analytical perspective, it is unnecessary because a reference spectrum can be recorded and archived in a few seconds by FASSST.

Figure 4 also shows that as  $B$  decreases, there are more thermally populated transitions and the lines are more closely spaced and weaker. Calculations show that the average spacing of rotational lines becomes equal to the Doppler width for molecules whose rotational constants are ~0.1 GHz. Although the relationship between rotational constants (which are inversely proportional to the moments of inertia) and the molecular mass  $M$  depends on the distribution of the atomic masses in the molecule, the moment of inertia of a spherical mass distribution of radius  $R$  with constant mass density grows

as  $R^5$  and  $M^2$ . For molecules of mass density similar to nitric acid, the rotational constants are ~0.1 GHz for molecules of mass ~1000 amu.

Figure 5 also illustrates another important feature of rotational spectra in the submillimeter region: the contributions from pure rotational transitions in excited vibrational states. Because methyl formate has larger rotational constants  $A$ ,  $B$ , and  $C$  than nitric acid, it has a sparser pure rotational spectrum. Because it has low-lying ( $<kT$ ) torsional and vibrational states, however, many of these contribute spectral peaks of similar intensity to that of the ground state, providing the much denser spectrum shown in the figure. It is likely that molecules of 1000 amu will have many low-lying, thermally populated states, thereby leading to a more congested spectrum than in the simple estimate above. On the other hand, molecules of 1000 amu made of atoms heavier than nitric acid will have larger rotational constants and less dense spectra. This large molecule limit is an interesting and as yet unexplored topic in rotational spectroscopy, which will ultimately place the limit on the mass and size of molecules which have highly specific rotational signatures.



typically, a few spectral lines (12, 13).

**Quantitative analysis.** Because the strengths of the molecular rotational transitions depend upon the permanent molecular dipole moment and angular momentum quantum mechanics, measured fractional absorption can be translated into absolute concentration by Equation 2 in the Box on the previous page and calculation of the partition function. Whereas rotational partition functions are straightforward to calculate, large molecules can have significant vibrational partition functions with significant contributions from largely unknown, low-lying vibrational modes. In these cases the calculations should be verified experimentally with known samples.

Most important, because of the high resolution of FASSST spectra, any of many isolated rotational lines ordinarily can be

used for quantitative purposes, thus providing massive redundancy and eliminating the possibilities of contributions from interfering and overlapping lines. For example, in the opening art, any of more than 100 lines could be used to determine the concentration. In real systems, moderate efforts at establishing the partition functions and fractional absorption of the submillimeter power should result in a quantitative uncertainty of ~10%, whereas 1% should be achievable for most species with modest effort.

### Possibilities

The system described above has been configured as a general-purpose laboratory instrument, with high-resolution spectroscopic capabilities. For many applications, modifications are appropriate.

For analytical purposes that require identification rather than state-of-the-art spectroscopic measurement, the frequency calibration requirements can be relaxed significantly, resulting in a smaller and more compact system. For example, frequency measurement accurate to a Doppler broadened linewidth would still leave  $10^5$  distinct channels for identification rather than the  $10^6$  channels of the system shown in Figure 1. This significantly reduces the power supply stability and FP size requirements. Additionally, for applications that do not require maximum sensitivity and spectral coverage, the system has an all solid-state analogue (FASSST-SS) based on chirped GUNN oscillators and Schottky diode detectors.

The sensitivity and selectivity of a FASSST system is optimal when the sam-

ple of asymmetry of the molecule and angular momentum projection quantum numbers (14). However, in the symmetric top limit (in which two of the rotational constants are equal),  $W_{J,K}(b_p) = K^2$  (in which  $K$  is the projection of  $J$  onto the molecular symmetry axis), and it is possible to use this relation along with the dipole selection rule  $J \rightarrow J+1$  to illustrate the general character of rotational spectra. In this symmetric top limit, it is straightforward to show that the values of  $J$  and  $v$  for which rotational lines are strongest are given by

$$J_{\text{opt}} \sim 5(T/B)^{1/2} \quad (5)$$

and

$$v_{\text{opt}} \sim 2B + 11(BT)^{1/2} \quad (6)$$

in which  $B$  is a rotational constant in gigahertz (14).

Figure 4 plots the absorption coefficients at 300 K for the  $K=0$  component of each  $J \rightarrow J+1$  transition for symmetric tops of various  $B$  values. For rigid symmetric tops, the  $K \neq 0$  components are degenerate with the  $K=0$  transitions, but for real molecules, the components are slightly (a few megahertz) displaced due to centrifugal distortion effects. For asymmetric tops, the  $K \neq 0$  components

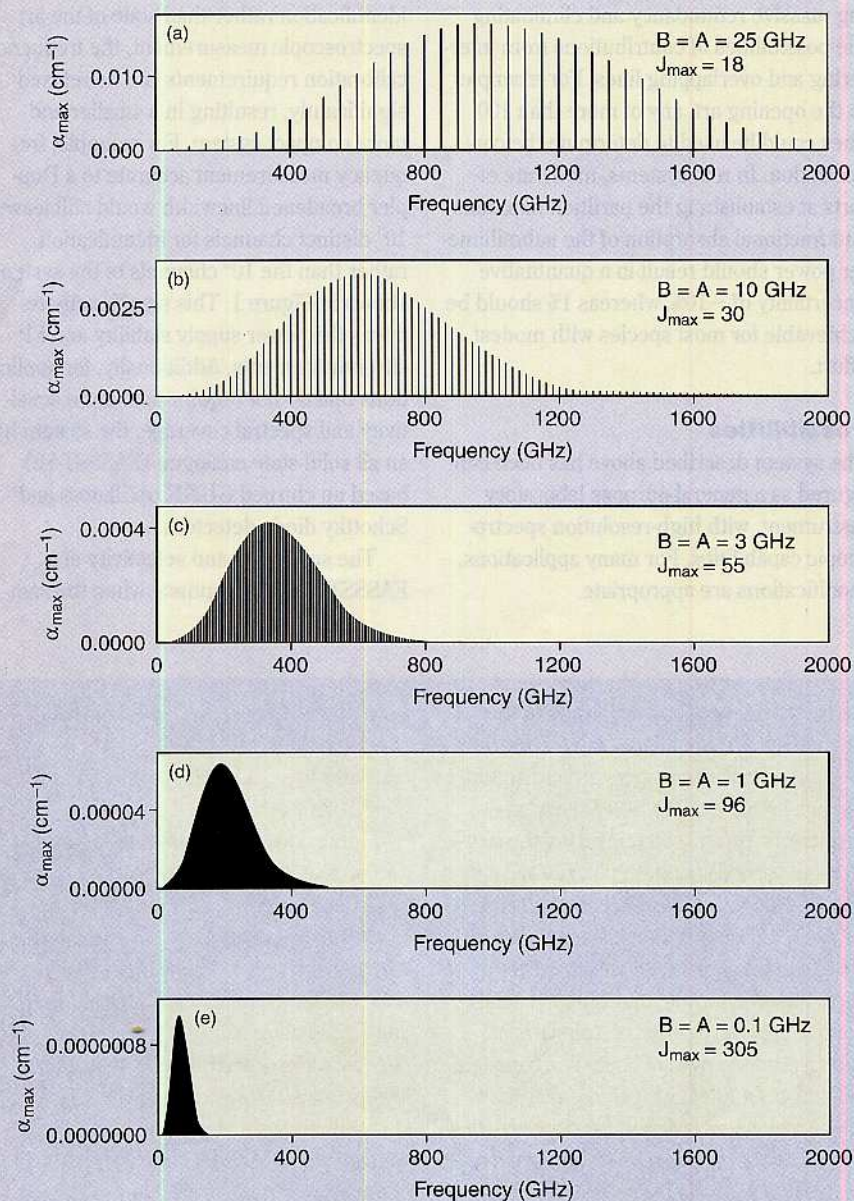
are more widely spread according to their asymmetry and Equation 4, but, on average, they have similar transition strengths. Additionally, because of the lower symmetry of asymmetric rotors, components of the dipole moment can exist along each axis, and a new set of selection rules and spectra will appear for each. Although this can lead to a spectrum of great complexity, the character of the symmetric tops is representative of the average spectral density, distribution in frequency, and strength of lines. The complete spectral assignment of asymmetric rotors can be a complex task, but from an analytical perspective, it is unnecessary because a reference spectrum can be recorded and archived in a few seconds by FASSST.

Figure 4 also shows that as  $B$  decreases, there are more thermally populated transitions and the lines are more closely spaced and weaker. Calculations show that the average spacing of rotational lines becomes equal to the Doppler width for molecules whose rotational constants are ~0.1 GHz. Although the relationship between rotational constants (which are inversely proportional to the moments of inertia) and the molecular mass  $M$  depends on the distribution of the atomic masses in the molecule, the moment of inertia of a spherical mass distribution of radius  $R$  with constant mass density grows

as  $R^5$  and  $M^2$ . For molecules of mass density similar to nitric acid, the rotational constants are ~0.1 GHz for molecules of mass ~1000 amu.

Figure 5 also illustrates another important feature of rotational spectra in the submillimeter region: the contributions from pure rotational transitions in excited vibrational states. Because methyl formate has larger rotational constants  $A$ ,  $B$ , and  $C$  than nitric acid, it has a sparser pure rotational spectrum. Because it has low-lying ( $<kT$ ) torsional and vibrational states, however, many of these contribute spectral peaks of similar intensity to that of the ground state, providing the much denser spectrum shown in the figure. It is likely that molecules of 1000 amu will have many low-lying, thermally populated states, thereby leading to a more congested spectrum than in the simple estimate above. On the other hand, molecules of 1000 amu made of atoms heavier than nitric acid will have larger rotational constants and less dense spectra. This large molecule limit is an interesting and as yet unexplored topic in rotational spectroscopy, which will ultimately place the limit on the mass and size of molecules which have highly specific rotational signatures.





**Figure 4. Calculated absorption coefficients as a function of frequency for symmetric and near-symmetric tops ( $K = 0$ ).**

Similar molecules include ethylene oxide (25 GHz), difluoroethane (10 GHz), norbornadiene (3 GHz), and fluorobenzene chromiumtricarbonyl (1 GHz).

ple pressure is 10–100 mTorr. It is common in many analytical applications to introduce samples into an instrument that changes the physical condition of the sample before the measurement occurs. For example, pressures in mass spectrometers are typically  $<10^{-5}$  Torr. These same techniques, including preconcentration methods, which have been developed for a wide array of analytical applications, can also be

used with FASSST systems.

The existing software that is used for the calibration of the FP fringes is based on the automated assignment of a known reference gas. This algorithm, which is very robust, can easily be extended to compare a library of reference gases for their identification and quantification. As the spectra in the figures show, the information content of the high-resolution FASSST spectra

is very high, and identification and quantification, even in relatively complex mixtures, is possible. Because absolute absorption coefficients for rotational transitions can be accurately calculated from measured dipole moments, the recovery of absolute concentrations is also straightforward.

Studying the rotational structure of molecular spectra has ordinarily been limited to relatively small molecules. In the IR, the rotational structure is ordinarily obscured by Doppler broadening for molecules with more than 5–10 atoms. In the microwave, measurement of the large number of rotational lines of heavier species is incompatible with the relatively slow systems used previously. Because rotationally resolved spectra provide absolute specificity even in complex mixtures, the extension of FASSST to large molecules with other physical properties that are similar will be important. Accordingly, we feel that the study of heavy organic and biological species with the FASSST system is a particularly exciting scientific opportunity.

Under most circumstances, sensitivity is proportional to the effective path length of the system. By using White-type cells or other multiple pass/cavity schemes, about two orders of magnitude improvement in sensitivity is obtainable. Also, the amplitude noise properties of BWOs are not well characterized in the spectral region that is the fundamental of the FASSST signal detection channel (100 kHz). It is probable that significantly greater system S/N (currently  $10^7$  for 1 s of integration) can be obtained.

For many applications, it is advantageous to combine GC with a spectroscopic technique, such as IR or MS. Because the recording time of FASSST spectra is shorter than the separation time on an analytical column, the output of the column can be connected directly to the absorption cell of the spectrometer. In addition, because the optimum sensitivity of FASSST occurs at a much lower pressure (10 mTorr) than that of IR or optical systems, significantly smaller sample separations from the column are required.

We would like to thank the Alexander von Humboldt Foundation for a fellowship (S. A.) and a Max Planck Prize (F.C.D.). We would also like



# Search and Conquer your information needs

SEARCH

## FOR FREE!

**ACS Web Editions now offer expanded search and retrieval of chemical information.**

Introducing a significant new free service for visitors to any ACS Web Edition home page. Information seekers can search by title and author across the table of contents of the entire Web Edition archive, (from 1996 to the most recent issue).

- A search can be applied to just one, several, or all 26 Web Editions.
- Search results will show full bibliographic citation details, including *journal and article title, author(s), issue, year, and page numbers*.
- All searches include any articles posted in *Articles ASAP*.
- Users of the cross-journal search feature can then connect directly to the abstract or full-text of the article if they have a current subscription to the journal in which the article appears.
- Non-subscribers can order the article through the convenient new single article sales service, *Articles on Command*.

For more information, visit  
**<http://pubs.acs.org>**



**Web Editions**  
ACS PUBLICATIONS

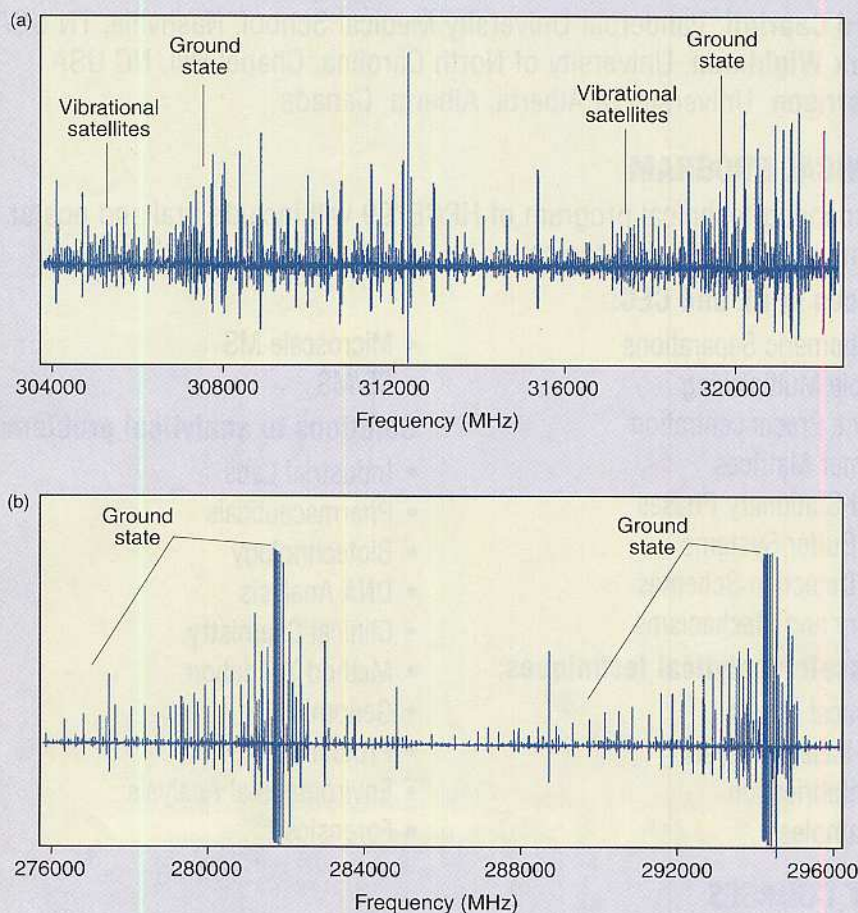


**Figure 5. FASSST spectra for (a) methyl formate, a molecule with many low lying vibrational and torsional states and (b) nitric acid, a molecule with all vibrational states lying above 2kT.**

For nitric acid, strong  $K = 0$  bandheads can be seen near 282 and 295 GHz, with the systematically spaced lines of decreasing intensity at lower frequency being the  $K \neq 0$  components.

to thank Richard McCreery for his useful comments about the manuscript. This work has also been supported by the Air Force Office of Scientific Research, the Army Research Office, and NASA.

## References

- (1) Townes, C. H.; Schawlow, A. L. *Microwave Spectroscopy*; McGraw-Hill Dover Publications, Inc.: New York, 1955. chapter 18.
- (2) Clement, R. E.; Yang, P. W. *Anal. Chem.* **1997**, 69, 251 R.
- (3) Fox, D. L. *Anal. Chem.* **1997**, 69, 1 R.
- (4) Putley, E. H. *Applied Optics* **1990**, 4, 649.
- (5) Petkie, D. T. et al *Rev. Sci. Instrum.* **1997**, 68, 1675.
- (6) Dryagin, Y. A. *Izv. VUZ. Radiofizika* **1970**, 13, 141.
- (7) Convert, G.; Yeou, T.; Pasty, B. In *Millimeter Waves*; Polytechnic Press: Brooklyn, 1959.
- (8) Karp, A. *Proc. L.R.E.* **1957**, 45, 496.
- (9) Robson, P. N. *Coherent Sources Using Electron Beams*; North-Holland: Amsterdam, 1967.
- (10) Bell, W.; Duxbury, G.; Stuart, D. D. *J. Mol. Spectrosc.* **1992**, 152, 283.
- (11) Brown, S. D.; Sum, S. T.; Despagne, F. *Anal. Chem.* **1996**, 68, 21 R.
- (12) Winniewisser, G.; Herbst, E. *Rep. Prog. Phys.* **1993**, 56, 1209.
- (13) Dickens, J. E. et al *ApJ.* **1997**, 489, 753.
- (14) Gordy, W.; Cook, R. L. *Microwave Molecular Spectra*, Third ed.; John Wiley & Sons: New York, 1984.

Sieghard Albert is a research fellow at Ohio State University. Douglas T. Petkie is an assistant professor at Ohio Northern University. Ryan P. A. Bettens is a research fellow at the Australian National University. Sergei P. Belov is a research scientist at Universitat Koln (Germany). Frank C. De Lucia is a professor at Ohio State University. Address correspondence about this article to De Lucia at the Department of Physics, Ohio State University, Columbus, OH 43210 ([fcd@mps.ohio-state.edu](mailto:fcd@mps.ohio-state.edu)).